

## Au Nanoparticles Prepared by Physical Method on Si and Sapphire Substrates for Biosensor Applications

J. Spadavecchia,<sup>†</sup> P. Prete,<sup>†</sup> N. Lovergine,<sup>‡</sup> L. Tapfer,<sup>§</sup> and R. Rella<sup>\*,†</sup>

*Istituto per la Microelettronica e i Microsistemi (IMM–CNR), Sezione di Lecce, Via Arnesano, I-73100 Lecce, Italy, Dipartimento di Ingegneria dell'Innovazione, Università di Lecce, Via Arnesano, I-73100 Lecce, Italy, and ENEA/UTS-MAT, Centro Ricerche di Brindisi, Strada Statale 7 "Appia", km 713+700, I-72100 Brindisi, Italy*

*Received: June 14, 2005; In Final Form: August 3, 2005*

Gold nanoparticles heavily functionalized with oligonucleotides have been used in a variety of DNA detection methods. The optical properties of three-dimensional aggregates of Au nanoparticles in solution or deposited onto suitable surfaces have been analyzed to detect hybridization processes of specific DNA sequences as possible alternatives to fluorescent labeling methods. This paper reports on the preparation of gold nanoparticles directly deposited onto the surface of silicon (Si) and sapphire (Al<sub>2</sub>O<sub>3</sub>) substrates by a physical methodology, consisting in the thermal evaporation of a thin Au film and its successive annealing. The method guarantees the preparation of monodispersed single-crystal Au nanoparticles with a strong surface plasmon resonance (SPR) peak centered at about 540 nm. We show that the changes of SPR excitation before and after DNA functionalization and subsequent hybridization of Au nanoparticles immobilized onto Si and Al<sub>2</sub>O<sub>3</sub> substrates can be exploited to fabricate specific biosensors devices in solid phase.

Development of simple and reliable protocols for the immobilization onto solid substrates of DNA oligonucleotides are beginning to assume an important role in biotechnological applications. To this purpose, Au nanoparticles heavily functionalized with oligonucleotides have been used in a variety of DNA detection methods.<sup>1–3</sup> The optical properties of three-dimensional aggregates of Au nanoparticles in solutions<sup>4,5</sup> or deposited onto suitable surfaces have been analyzed to detect hybridization processes of specific DNA sequences, as possible alternatives to fluorescent labeling methods.<sup>6,7</sup> Most widely used methods for synthesizing Au nanoparticles are based on solution chemical reactions, yielding nanoparticle colloids.<sup>8,9</sup>

This paper reports on the preparation of Au nanoparticles directly onto the surface of silicon (Si) and sapphire (Al<sub>2</sub>O<sub>3</sub>) substrates by a physical methodology, consisting of the thermal evaporation of a thin Au film and its successive annealing. The method guarantees the preparation of monomodal Au nanoparticles with strong surface plasmon resonance (SPR).<sup>10</sup> We show that the changes of SPR excitation before and after functionalization and subsequent hybridization of Au nanoparticles immobilized onto Si and Al<sub>2</sub>O<sub>3</sub> substrates can be exploited to fabricate specific biosensors in solid phase. The DNA functionalization and hybridization of as-prepared Au nanoparticles were achieved with *Fusarium* thio-DNA (5'HS(T)15 ATCCCTCAAAAAGTCCGCT-3') and Trichotecenes complementary DNA (AGC GGC AGT TTT TGA) sequences,

respectively. Trichotecenes is known as one of the most important *Fusarium* mycotoxins, that can frequently occur at biologically significant concentrations in cereals and to cause a variety of acute and chronic animal and human diseases.

Au nanoparticles were prepared on both p-type (100)-oriented Si and (0001)-oriented Al<sub>2</sub>O<sub>3</sub> substrates (10 × 10 mm<sup>2</sup> in size) cleaved from commercial wafers. Both Si and Al<sub>2</sub>O<sub>3</sub> substrates were first degreased by rinsing in boiling acetone for 20 min, cleaned in 2-propanol vapors for 1 h and finally dried under pure nitrogen (N<sub>2</sub>) flow. The substrates were then loaded in a Joule evaporator UHV chamber for the subsequent deposition of a Au thin film. The Au film thickness ranged between 1 and 4 nm, the evaporation rate being around 0.02 nm/s. After evaporation the samples were loaded into the quartz chamber of a horizontal tubular resistance furnace for annealing under inert atmosphere. Annealing experiments were performed for 20 min at 814 °C under 200 cm<sup>3</sup>/min pure N<sub>2</sub> flow. This thermal treatment allows the Au thin film to self-assemble into a dense and uniform (across the substrate area) array of nanoparticles. The morphology, size, and crystalline structure of Au nanoparticles were characterized by field emission scanning electron microscopy (FE-SEM) and X-ray diffraction (XRD), respectively. FE-SEM observations were performed using a JEOL 6500F microscope, with a 15 kV electron beam accelerating voltage. XRD measurements were performed in both Bragg ( $\theta$ -2 $\theta$  scan) and glancing incidence (GIXRD) geometry. GIXRD spectra were recorded by using a high-resolution X-ray diffractometer (HRD3000 Ital Structures) in parallel beam optic configuration (Max-Flux Optical System).

\* Corresponding author. E-mail: roberto.rella@ime.le.cnr.it.

<sup>†</sup> Istituto per la Microelettronica e i Microsistemi.

<sup>‡</sup> Università di Lecce.

<sup>§</sup> ENEA/UTS-MAT.

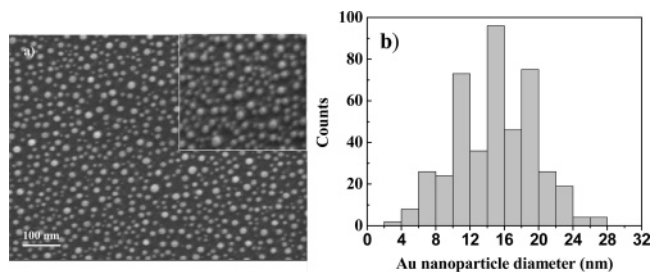


**Figure 1.** (a) Plan-view FE-SEM micrograph of a 2 nm thin Au film on (100)Si after annealing at 814 °C. The inset shows a micrograph taken with the sample tilted 40° with respect to the detector. (b) Histogram of the Au nanoparticle diameter counts, measured from the plan-view image in (a).

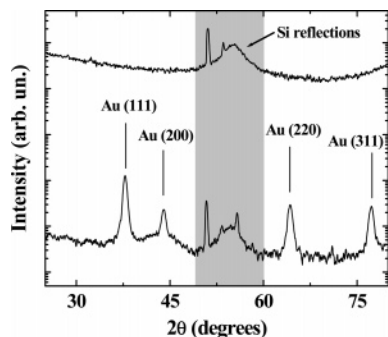


**Figure 2.** GIXRD spectra of a 4 nm thin Au film on (100)Si after annealing at 814 °C (lower curve) and of a bare (100)Si substrate (upper curve). The gray area in the diagram indicates the angular region where reflections due to Si appear. Crystallographic identifications of the Au peaks are also indicated in the figure.

Figure 1a shows the morphology of a 2 nm thin Au deposit on Si after the annealing treatment. Au nanoparticles with a density of around  $1.8 \times 10^{11} \text{ cm}^{-2}$  appear to have formed on the Si surface, their shape being droplet-like, as it shows from the 40° tilted FE-SEM image reported in the Figure inset. Figure 1b reports a count histogram of the Au nanoparticle diameters, as measured from the plan-view image of Figure 1a, demonstrating that the nanoparticles are monomodal with an average diameter of 15.8 nm. Further quantitative analyses performed on similarly treated samples confirmed this conclusion, showing that for a 2 nm thin Au deposit on Si the nanoparticle density and average diameter vary in the  $10^{10}$ – $10^{11} \text{ cm}^{-2}$  range and 14–19 nm interval, respectively. Noteworthy, increasing the thickness of the initial Au film leads to a slight increase of the nanoparticle average size.

Figure 2 shows the GIXRD spectrum of a 4 nm thin Au deposit on (100)Si sample after annealing, along with that of a bare Si substrate. FE-SEM observations of the sample surface after annealing confirmed the formation of nanoparticles, similarly to what is shown in Figure 1. The sample GIXRD spectrum in Figure 2 shows the occurrence of diffraction peaks ascribable to solid Au (fcc phase), indicating that as-formed nanoparticles are indeed composed of elemental Au. Diffraction experiments performed in the Bragg geometry showed that the Au nanoparticles are mostly (111)-oriented with respect to (100)Si. The widths of the Au peaks in the GIXRD pattern of Figure 2 allows to estimate a Au crystallite average size  $\sim 15.6$  nm, i.e., not far from the 19.9 nm value of the nanoparticle average diameter derived from FE-SEM observations.

Analogously, XRD experiments ( $\theta$ -2 $\theta$  scan) performed on (0001)Al<sub>2</sub>O<sub>3</sub> samples evidenced that Au nanoparticles are invariably (111)-oriented with respect to the substrate. Due to the difficulty of performing FE-SEM observations on highly

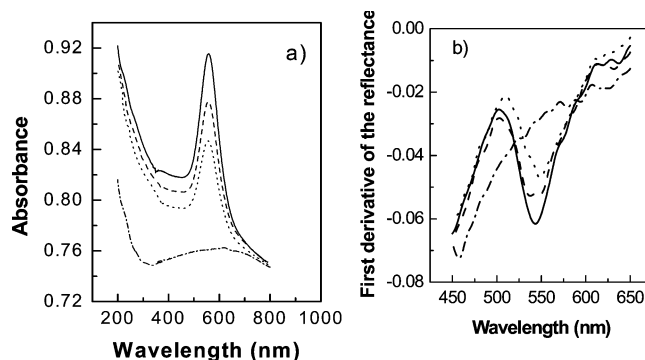


**Figure 3.** Absorption spectra of Au nanoparticles on Al<sub>2</sub>O<sub>3</sub> (a) and first derivative of the reflectivity spectra of Au nanoparticles on Si (b). Different curves correspond to functionalized (dash line) and hybridization (dot line) samples and to as-prepared Au nanoparticles (solid line). Dot-dashed lines correspond to Al<sub>2</sub>O<sub>3</sub> and Si substrates without Au.

insulating samples, the size of Au nanoparticles formed on Al<sub>2</sub>O<sub>3</sub> was estimated from the width of the Au (111) peak in the diffraction spectra. For a 3 nm thin Au film, the crystallite size after sample annealing turned out to be  $\sim 10.6$  nm.

The optical absorption of the Au nanoparticle thin layer deposited onto Al<sub>2</sub>O<sub>3</sub> was characterized by UV–visible spectrophotometry, while reflectivity measurements were performed for Au nanoparticles prepared on Si. Figure 3a reports the optical absorption spectrum of Au nanoparticles (crystallite size 10.4 nm) prepared on Al<sub>2</sub>O<sub>3</sub>. The spectrum displays a strong resonance peak at around 540 nm caused by SPR of individual nanoparticles,<sup>11</sup> in addition to indicating that the nanoparticles are isolated from each other and sufficiently monomodal.

The successive functionalization of Au nanoparticles has been performed with a single-stranded modified DNA. In particular 10  $\mu\text{L}$  of 25  $\mu\text{M}$  HS-ssDNA solutions was prepared (in 10mM tris 10mM NaCl buffer, pH 7.2), and droplets of this solution were deposited onto the surface of the sample and left to react for at least 18 h at RT in a humid environment to prevent the droplets from drying out. Successively, the substrate was soaked in deionized water for some minutes and rinsed with water to remove probes not absorbed. The sensing layer was then ready to be used for hybridization. To this purpose the sample was immersed for 18 h in a 25  $\mu\text{M}$  complementary oligonucleotide in PBS (phosphate buffer solution pH 7.4). After rinsing in deionized water, the sensor chip thus obtained was ready for optical absorption measurements. Figure 3a reports the observed changes of the SPR band after functionalization and hybridization with the DNA probe and complementary DNA target. Washing repeatedly in the buffer solution the Al<sub>2</sub>O<sub>3</sub> sample containing the as deposited gold nanoparticles, any change in the SPR absorption peak is monitored thus demonstrating a good adhesion of the nanoparticles onto the Al<sub>2</sub>O<sub>3</sub> substrate. On the contrary, a significant intensity decrease in the SPR absorption band appears after the functionalization. This decrease is due to the formation of chemical bonds between the HS-dssDNA probes and the Au nanoparticles after the functionalization and their successive bonding with the complementary DNA target (hybridization). These results clearly show that the optical absorbance of a Au nanoparticle monolayer is sensitive to the refractive index change caused by the DNA/DNA binding events at the surface of individual nanoparticles. Similar interaction mechanisms originate the changes in the reflectivity spectra observed for DNA-functionalized Au nanoparticles prepared on Si. Figure 3b shows the first derivative of the sample reflectivity in the UV–visible spectral range of both as-prepared Au

nanoparticles and after their subsequent DNA functionalization and hybridization. Also in this case variations in the reflectivity spectra can be attributed to the change in the refractive index at the surface of each nanoparticle.

In conclusion, monomodal Au nanoparticles with strong SPR can be prepared onto suitable substrates by a simple physical methodology for optical biosensor applications. Food quality control applications are potentially possible as well as applications in other fields, like medicine, environment, etc. Further study will be performed in order to give a metrics of the system in terms of sensitivity, selectivity, reproducibility, and stability of the sensor chip.

## References and Notes

- (1) Mirkin, C. A.; Letsinger, R. L.; Mucic, R. C.; Storhoff J. J. *Nature* **1996**, 382, 607.
- (2) Soweth, C. J.; Caldwell, W. B.; Peng, X.; Alivisatos, A. P.; Shultz, R. G. *Angew. Chem., Int. Ed. Engl.* **1999**, 38, 1808–1812.
- (3) Otsuka, H.; Akiyama, Y.; Nagasaki, Y.; Kataoka, K. *J. Am. Chem. Soc.* **2001**, 123, 8226.
- (4) Storhoff, J. J.; Elghanian, R.; Mucic, R. C.; Mirkin, C. A.; Letsinger, R. L. *J. Am. Chem. Soc.* **1998**, 120, 1959–1964.
- (5) Elghanian, R.; Storhoff, J. J.; Mucic, R. C.; Letsinger, R. L.; Mirkin, C. A. *Science* **1997**, 277, 1078–1081.
- (6) He, L.; Musick, M. D.; Nicewarner, S. R.; Salinos, F. G.; Benkovic, S. J.; Natan, M. J.; Keating, C. D. *J. Am. Chem. Soc.* **2000**, 122, 9071–9077.
- (7) Tarton, T. A.; Mucic, R. C.; Mirkin, C. A.; Letsinger, R. L. *J. Am. Chem. Soc.* **2000**, 122, 6305–6306.
- (8) Jana, N. R.; Gearheart, L.; Murphy, C. J. *J. Phys. Chem. B* **2001**, 105, 4065.
- (9) Walker, C. H.; St. John, J. V.; Wisian-Neilson, P. *J. Am. Chem. Soc.* **2001**, 123, 3846.
- (10) Kreibig, U.; Vollmer, M. *Optical Properties of Metal Clusters*, Springer-Verlag: Berlin 1996).
- (11) Kim, Y. J.; Johnson, R. C.; Hupp, J. T. *Nanolett.* **2001**, 1, 165.